Refractive accuracy with light-adjustable intraocular lenses

Eloy A. Villegas, PhD, Encarna Alcon, MSc, Elena Rubio, MD, José M. Marín, MD, PhD, Pablo Artal, PhD

PURPOSE: To evaluate efficacy, predictability, and stability of refractive treatments using light-adjustable intraocular lenses (IOLs).

SETTING: University Hospital Virgen de la Arrixaca, Murcia, Spain.

DESIGN: Prospective nonrandomized clinical trial.

METHODS: Eyes with a light-adjustable IOL (LAL) were treated with spatial intensity profiles to correct refractive errors. The effective changes in refraction in the light-adjustable IOL after every treatment were estimated by subtracting those in the whole eye and the cornea, which were measured with a Hartmann-Shack sensor and a corneal topographer, respectively. The refractive changes in the whole eye and light-adjustable IOL, manifest refraction, and visual acuity were obtained after every light treatment and at the 3-, 6-, and 12-month follow-ups.

RESULTS: The study enrolled 53 eyes (49 patients). Each tested light spatial pattern (5 spherical; 3 astigmatic) produced a different refractive change ($P<.01$). The combination of 2 light adjustments induced a maximum change in spherical power of the light-adjustable IOL of between −1.98 diopters (D) and +2.30 D and in astigmatism of up to −2.68 D with axis errors below 9 degrees. Intersubject variability (standard deviation) ranged between 0.10 D and 0.40 D. The 2 required lock-in procedures induced a small myopic shift (range +0.01 to +0.57 D) that depended on previous adjustments.

CONCLUSIONS: Light-adjustable IOL implantation achieved accurate refractive outcomes (around emmetropia) with good uncorrected distance visual acuity, which remained stable over time. Further refinements in nomograms and in the treatment's protocol would improve the predictability of refractive and visual outcomes with these IOLs.

Financial Disclosure: No author has a financial or proprietary interest in any material or method mentioned.

J Cataract Refract Surg 2014; 40:1075–1084 © 2014 ASCRS and ESCRS

Supplemental material available at www.jcrsjournal.org.

Cataract surgery has become a successful procedure to restore normal vision. Although phacoemulsification and foldable intraocular lens (IOL) implantation has largely improved this surgery, the calculation of the IOL power to obtain emmetropia (refraction below ±0.50 diopter [D]) continues to be a problem. The current predictions using regression formulas are sometimes not accurate as a result of errors in preoperative biometry and keratometry measurements, surgically induced corneal astigmatism, or variations in axial positions of the IOL. Most clinical studies report errors in IOL power calculation of approximately 0.50 D on average; however, the standard deviation (SD) is 0.50 D or higher.[1–5]

Approximately 50% of patients with IOLs have a residual spherical equivalent (SE) higher than 0.50 D. Furthermore, the highest refractive errors after cataract surgery have been in eyes with previous corneal refractive surgery. Despite specific formulas[6] and ray-tracing procedures[7,8] that have been developed to improve these results, refractive errors of more than 0.50 D are common in pseudophakic eyes with previous laser refractive surgery.

On the other hand, postoperative astigmatism that is mainly the result of the preoperative corneal shape and/or induced by corneal incisions reduces the optical and visual quality postoperatively. Previous studies[9,10] report preoperative mean corneal astigmatism values of approximately 0.75 D ± 0.50 (SD). However, one quarter of eyes have preoperative astigmatism of 1.50 D or higher.[11] Corneal incisions change the amount and the orientation of the

http://dx.doi.org/10.1016/j.jcrs.2013.10.046

preoperative astigmatism.[8,10,12–14] Although toric IOL implantation[15–17] is an option to correct corneal astigmatism, it does not correct that induced by surgery.

Light-adjustable IOLs can correct remaining refractive errors after cataract surgery. Appropriate spatial light intensity patterns used to irradiate the IOLs after implantation modify their shape, allowing the correction of defocus and astigmatism.[18,19] Clinical studies[20–23] found that after cataract surgery, light-adjustable IOLs irradiated with the appropriate spatial patterns successfully corrected residual myopia, hyperopia, and astigmatism.

However, the behavior of light-adjustable IOLs in the human eye and the accuracy of the corrections have not been reported. In this study, we used wavefront aberration measurements from the whole eye and from the cornea in patients with light-adjustable IOLs to estimate the refractive changes and stability in the whole eye and in the light-adjustable IOL after treatments with different profiles to correct myopia, hyperopia, and astigmatism. The evolution of manifest refraction and visual acuity and the stability of refractions 3, 6, and 12 months postoperatively were also studied.

PATIENTS AND METHODS

All clinical examinations and surgery were performed at the Ophthalmology Department, Virgen de la Arrixaca Hospital, Murcia, Spain. The hospital's ethics committee approved this study, which followed the tenets of the Declaration of Helsinki. After receiving an explanation of the nature and possible consequences of the surgery, all patients provided informed consent.

Submitted: September 7, 2013.
Final revision submitted: October 22, 2013.
Accepted: October 26, 2013.

From Laboratorio de Optica (Villegas, Alcon, Artal), Departamento de Física, Universidad de Murcia, and Servicio de Oftalmología (Rubio, Marín), Hospital Universitario Virgen de la Arrixaca El Palmar, Murcia, Spain.

Supported by the Ministerio de Ciencia e Innovación (grants FIS2010-14926 and CSD2007-00013) and Fundación Séneca (Region de Murcia, Spain, grant 4524/GERM/06), Spain, and Calhoun Vision, Pasadena, California, USA.

Presented in part at the annual meeting of the Association for Research in Vision and Ophthalmology, Fort Lauderdale, Florida, USA, May 2009.

Corresponding author: Eloy A. Villegas, PhD, Laboratorio de Optica, Campus de Espinardo, Centro de Investigación en Optica y Nanofisica, Universidad de Murcia, 30100 Murcia, Spain. E-mail: villegas@um.es.

Light-Adjustable Intraocular Lens and Spatial Light Intensity Patterns

The light-adjustable IOL used in this study (LAL, Calhoun Vision, Inc.) contains photosensitive molecules that enable noninvasive postoperative adjustment of the optical power using ultraviolet (UV) light. The light-adjustable IOL material and performance have been described.[18,19,24] On irradiation with 365 nm UV light, the macromer molecules in the irradiated region are photopolymerized to form an interpenetrating network. This produces a concentration gradient between the irradiated area and nonirradiated area of the IOL that leads to diffusion of the remaining nonirradiated macromer into the irradiated areas; this induces a change in IOL shape, producing a power change. The posterior surface of the IOL has a UV light–filtering layer to provide protection to the retina against UV light during the irradiation procedure.

The defocus and astigmatism of the light-adjustable IOL after its implantation are modified by applying the appropriate spatially resolved irradiation profile with adequate irradiation (ie, beam intensity and duration). If refractive errors were not totally corrected with the first adjustment, a second one was performed after 2 or 3 days. The final part of the procedure consisted of 2 more visits, referred to as first lock-in and second lock-in. At these visits, the entire IOL was irradiated to polymerize remaining unreacted macromers. Thus, macromer diffusion is prevented and the IOL will be permanently stable.

The light-adjustable IOL is irradiated using a digital light-delivery system (Carl Zeiss Meditec AG) and is described elsewhere.[18,19,24] The digital light-delivery system consists of a UV light source, projection optics, and control interface built around a standard slitlamp. The light source is a mercury arc lamp with a band-pass interference filter that produces a narrow-wavelength beam with a center wavelength of 365 nm. The digital light-delivery system contains a pixelated digital mirror device that defines a specific high-resolution spatial intensity profile and then irradiates the light-adjustable IOL. To adjust the refraction of the patient, profiles to correct myopia, hyperopia, myopic astigmatism, or hyperopic astigmatism were used. Figure 1 shows these patterns with the irradiation conditions (intensity power, duration, and profile diameter) and number of eyes treated. In cases of emmetropia before adjustments, a neutral profile was applied to stabilize the IOL before the lock-in treatments.

Because of the limits of astigmatism correction with the light-adjustable IOL, patients with preoperative corneal astigmatism higher than 2.00 D were not included in the study. The IOL powers were selected based on internally optimized regression analysis with an A-constant of 119.3 to achieve a slight hyperopia (approximately +0.25 D) before the light adjustments were performed.

Surgical Technique

The same surgeon (J.M.M.) performed all surgeries. A 3.50 mm corneal incision was created in the temporal side in the right eye and in the nasal side in the left eye. Then, 0.5 mL of a dispersive ophthalmic viscosurgical device (OVD) (sodium hyaluronate 3.0%–chondroitin sulfate 4.0% [Viscoat]) was placed in the anterior chamber and a capsulorhexis of 5.5 mm or larger was created. The cataractous lens was extracted with the stop-and-chop phacoemulsification technique, after which 10 mg/mL of a cohesive

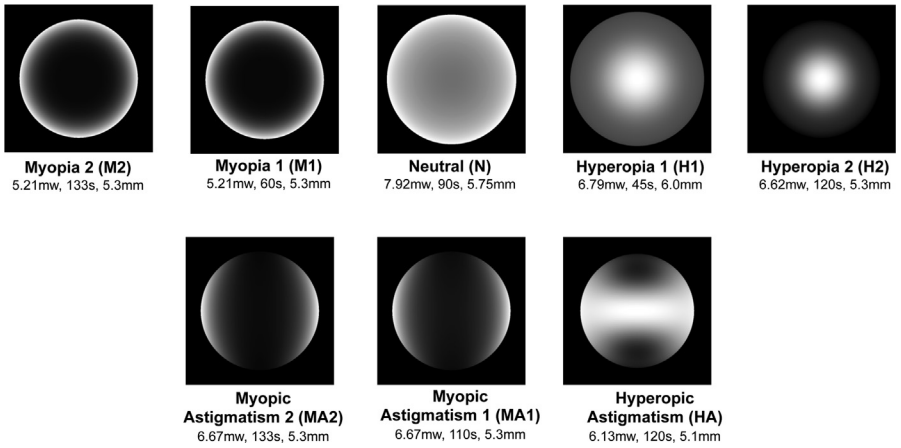

Figure 1. Spatial intensity profiles for hyperopic, myopic, astigmatic, and neutral adjustments. The irradiation dose is controlled with the power (mw), duration (s), and profile diameter (mm).

OVD (sodium hyaluronate 1.0% [Healon]) was placed in the anterior chamber. Next, the light-adjustable IOL was implanted in the capsular bag. The residual OVD was aspirated using a bimanual technique. The incision was not sutured. A steroidal antiinflammatory and antibiotic were applied to the eye. The patient was instructed to use glasses with UV protection until all light treatments were completed.

Treatment Schedule and Follow-up Visits

The visit schedule from the first adjustment to 1 year after the second lock-in was as follows: first adjustment, 2 weeks after surgery; second adjustment or first lock-in (depending on refractive evaluation), 2 to 3 days after the first adjustment; first or second lock-in, 2 to 3 days after second adjustment or first lock-in; second lock-in, 2 to 3 days after first lock-in; after second lock-in, 7 to 30 days; 3-month visit, 10 to 14 weeks after second lock-in; 6-month visit, 22 to 26 weeks after second lock-in; 1-year visit, 45 to 53 weeks after second lock-in. In patients with residual refraction after the first adjustment, a second adjustment was performed. In some cases, a neutral profile was also used in a second session to prevent possible refractive changes during lock-ins.

Patient Examinations

Preoperative tests were performed within 15 days before surgery. At all visits, the clinical examinations included slitlamp biomicroscopy, intraocular pressure, corneal topography, biometry, wavefront-guided refraction, and corrected (CDVA) and uncorrected (UDVA) distance visual acuities. In addition, the preoperative, primary adjustment, and 7-month postoperative examinations included ophthalmoscopy and retinal optical coherence tomography (OCT). Ocular wavefront measurements were taken at all postoperative visits.

Refractive Estimations

Wavefront aberrations in the eye were measured using a near-infrared Hartmann-Shack wavefront sensor built in the laboratory[25] and adapted to the clinical environment. This system has 188 microlenses for a 5.0 mm diameter pupil; the size of each microlens on the eye's pupil is 0.3 mm. The Hartmann-Shack images were recorded in a dark room to achieve a natural pupil diameter larger than 3.0 mm. Wavefront aberrations were expressed by Zernike coefficients for a 3.0 mm pupil.

The wavefront aberration in the anterior cornea was determined by ray tracing through the corneal surface. The geometry of the cornea was determined using a Placido-based

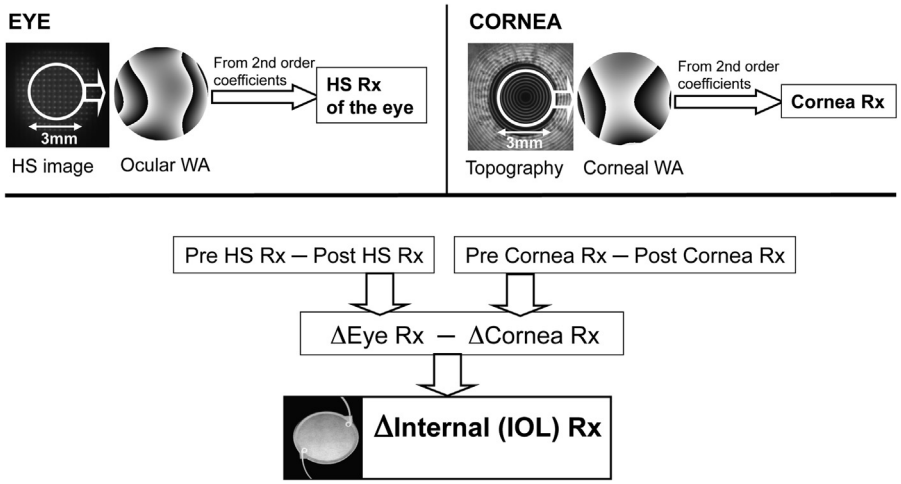

Figure 2. Calculations of changes (Δ) in refraction (Rx) after a treatment. *Upper*: First, the wavefront aberration (WA) of the cornea and the eye from topography and Hartmann-Shack measurements, respectively, were calculated for a 3.0 mm pupil diameter. Refractions were obtained from 2nd-order Zernike coefficients. *Lower*: The change in refraction was calculated as the difference between refraction before treatment (pre) and after treatment (post). Internal (IOL) variation in refraction was calculated as the subtraction of the cornea to the eye change. The subtractions were obtained using obliquely cross-cylinder calculations (IOL = intraocular lens).

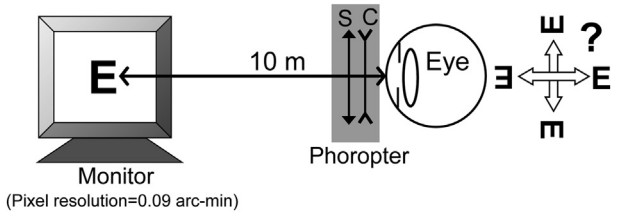

Figure 3. Subjective refinement of sphere from Hartmann-Shack refraction (arc-min = minutes of arc; C = cylinder; S = sphere).

corneal topographer (Atlas, software version 1.0.1.0, Carl Zeiss Meditec AG). This procedure has been described.[26,27] In summary, it consists of 2 steps. First, the corneal surface was described as a Zernike expansion from the values of elevations provided by the topographer. Then, the associated wavefront aberration was calculated by an exact ray-tracing procedure (Zemax Development Corp.) for a 3.0 mm pupil diameter. The distance between the center of the pupil and the corneal vertex was used to realign the corneal wavefront aberration to the pupil center so no errors were introduced in the alignment of corneal and internal aberrations.[28] Objective refractions for both the whole eye and the cornea were calculated from the 2nd-order Zernike coefficients by

$$C = \frac{-4\sqrt{6}\sqrt{Z(2,-2)^2 + Z(2,2)^2}}{r^2} \quad (1)$$

$$S = \frac{-4\sqrt{3}Z(2,0)}{r^2} - \frac{C}{2}$$

$$\text{Axis} = \frac{1}{2}\tan^{-1}\left(\frac{Z(2,-2)}{Z(2,2)}\right)$$

where C, S, and Axis are the cylinder, the sphere, and the cylinder orientation, respectively, of the refraction expressed in spherocylindrical form with negative cylinder, and Z(2,−2), Z(2,0), and Z(2,2) refer to the standard Zernike coefficients.[29] From 5 wavefront aberration measurements, the mean values of the refractions were calculated; their errors were expressed as the SD.

Figure 2 shows the procedure used to determine refractions from the Hartmann-Shack and corneal topography measurements and the changes in the whole eye, cornea, and IOL caused by the light treatments. The corneal refraction was defined as the corneal power and its astigmatism. The refraction changes induced by treatments were calculated as the difference between the refraction before treatment and the refraction after treatment measured at the next follow-up. To accurately estimate the subtraction of refractions, the cylinders were combined using the formulas of obliquely cross-cylinders as follows:

$$\tan 2\beta = \frac{c_2 \sin 2a}{c_1 + c_2 \cos 2a} \quad (2)$$

$$c = \frac{c_2 \sin 2a}{\sin 2\beta}$$

$$s = \frac{c_1 + c_2 - c}{2}$$

where c_1 and c_2 are the combined cylinders; a is the minimum angle between the axes; β and c are the axis orientation and the value of resulting cylinder, respectively; and s is the resulting sphere that must be added to the sphere values of the combined spherocylindrical forms. The angle of cylinder c_1 must be smaller than that of c_2, and the value of β is measured with respect to the axis of c_1. In the same way, the refraction changes of the internal optics of the eye (primarily of the light-adjustable IOL) were calculated by subtracting the anterior corneal refraction from the ocular refraction (Figure 2). Assuming a simple model for the eye with the cornea simplified to 1 surface, the internal optics of the eye is almost the same

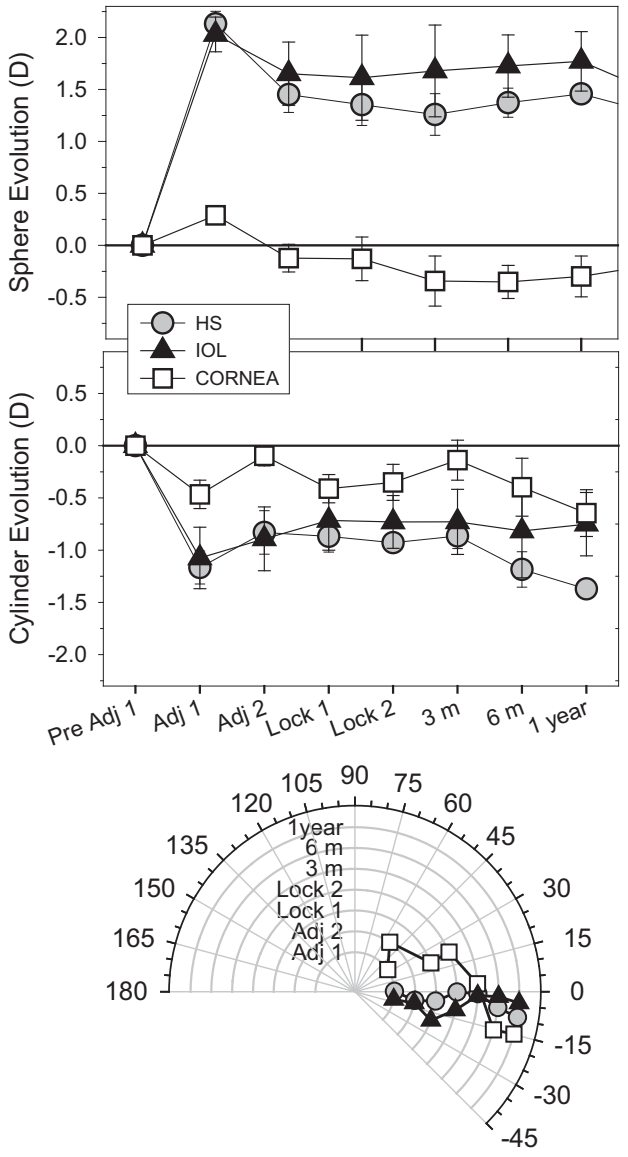

Figure 4. An example of the evolution of refraction changes (sphere, cylinder, and the axis orientation) in the eye and in the light-adjustable IOL in vivo with treatments and over time. First adjustment was astigmatic, and the second adjustment was myopic (Adj = adjustment; HS = Hartmann-Shack; IOL = intraocular lens).

Table 1A. Intraindividual mean values of refraction changes of the spherical profiles in the first adjustment.

Parameter	M2: 5 Samples (Mean ± SD*)	*P* Value†	M1: 5 Samples (Mean ± SD*)	*P* Value†	N: 5 Samples (Mean ± SD*)	*P* Value†	H1: 6 Samples (Mean ± SD*)	*P* Value†	H2: 5 Samples (Mean ± SD*)
Eye									
Sph (D)	−1.19 ± 0.20	.02	−0.79 ± 0.22	<.01	+0.49 ± 0.25	<.01	+0.87 ± 0.10	<.01	+1.58 ± 0.12
Cyl (D)	−0.20 ± 0.14	.26	−0.30 ± 0.13	.9	−0.31 ± 0.13	.65	−0.35 ± 0.13	.38	−0.27 ± 0.17
IOL									
Sph (D)	−1.19 ± 0.16	.06	−0.79 ± 0.37	<.01	+0.31 ± 0.28	<.01	+0.93 ± 0.20	<.01	+1.65 ± 0.16
Cyl (D)	−0.23 ± 0.10	.48	−0.29 ± 0.16	.58	−0.34 ± 0.12	.80	−0.33 ± 0.13	.64	−0.28 ± 0.16

Sph = sphere; Cyl = cylinder; IOL = intraocular lens; H1 and H2 = light profiles to correct hyperopia (Figure 1); M1 and M2 = light profiles to correct myopia (Figure 1); N = neutral light profile (Figure 1)
*Errors (variability) are expressed as the SD.
†Statistically significant difference between profiles is $P < .05$.

as that of the IOL. To calculate the effects of treatments on the eye and cornea, the refraction before treatment and that after treatment with the opposite sign were combined. The effect on the IOL was estimated by combining the refractive changes in the eye and those in the cornea with the opposite sign.

The difference between the axis direction in the preadjustment measurements and the orientation of the refraction change gives the axis error of the treatment. From equation 2, in astigmatic treatments, the uncorrected cylinder prescription as a function of axis error was also calculated.

The changes in refraction after the 2 lock-ins were also evaluated, with each lock-in assessed separately.

Subjective Refraction and Visual Acuity

A standard phoropter was used to determine the subjective refraction starting from the objective values; the values were rounded to steps of 0.25 D. For visual testing, a computer monitor with average luminance of 100 candelas/m^2 was placed 10 m from the patient (Figure 3). The tumbling "E" letter size was reduced (in steps of 0.09 arc minutes) up to the smallest letter the patient could see. In most patients, the optimum defocus was approximately 0.50 D lower than that of Hartmann-Shack due to the chromatic shift from infrared light in the wavefront sensor and the visible spectrum of the monitor. The CDVA and UDVA were measured and expressed as decimal units (ie, inverse of MAR).

RESULTS

Light-adjustable IOLs were implanted in 53 eyes of 49 patients. The power of implanted IOLs ranged from 18.0 to 25.0 D.

Figure 4 shows an example of the evolution of the refractive changes during the treatments. The first adjustment was astigmatic (HA) and the second was myopic (M2). The objective refraction variations in the eye and the IOL were similar, and the differences were mainly the result of small changes in the cornea. The first adjustment changes in the IOL were +2.10 D sphere and −1.10 D cylinder, and the second adjustment induced −0.50 D sphere. The IOL refraction was stable after lock-ins and 3, 6, and 12 months postoperatively. The orientation of the cylinder axes in the eye and in the IOL was similar and stable over time. In this case, the changes in the axis of the cornea were not important because the changes in corneal astigmatism were small.

Tables 1A and 1B and Figures 5 and 6 show the refractive changes produced by the light profiles in the first

Table 1B. Intraindividual mean values of refraction changes of the astigmatic profiles in the first adjustment.

Parameter	MA2: 10 Samples (Mean ± SD*)	*P* Value†	MA1: 8 Samples (Mean ± SD*)	*P* Value†	HA: 9 Samples (Mean ± SD*)
Eye					
Sph (D)	+0.61 ± 0.25	.68	+0.56 ± 0.17	<.01	+1.82 ± 0.34
Cyl (D)	−1.77 ± 0.43	<.01	−1.07 ± 0.25	.47	−1.15 ± 0.19
IOL					
Sph (D)	+0.59 ± 0.28	.96	+0.60 ± 0.40	<.01	+1.74 ± 0.35
Cyl (D)	−1.74 ± 0.40	<.01	−1.12 ± 0.26	.91	−1.14 ± 0.28

Sph = sphere; Cyl = cylinder; IOL = intraocular lens; HA = light profile to correct hyperopic astigmatism (Figure 1); MA1 and MA2 = light profiles to correct myopic astigmatism (Figure 1)
*Errors (variability) are expressed as the SD.
†Statistically significant difference between profiles is $P < .05$.

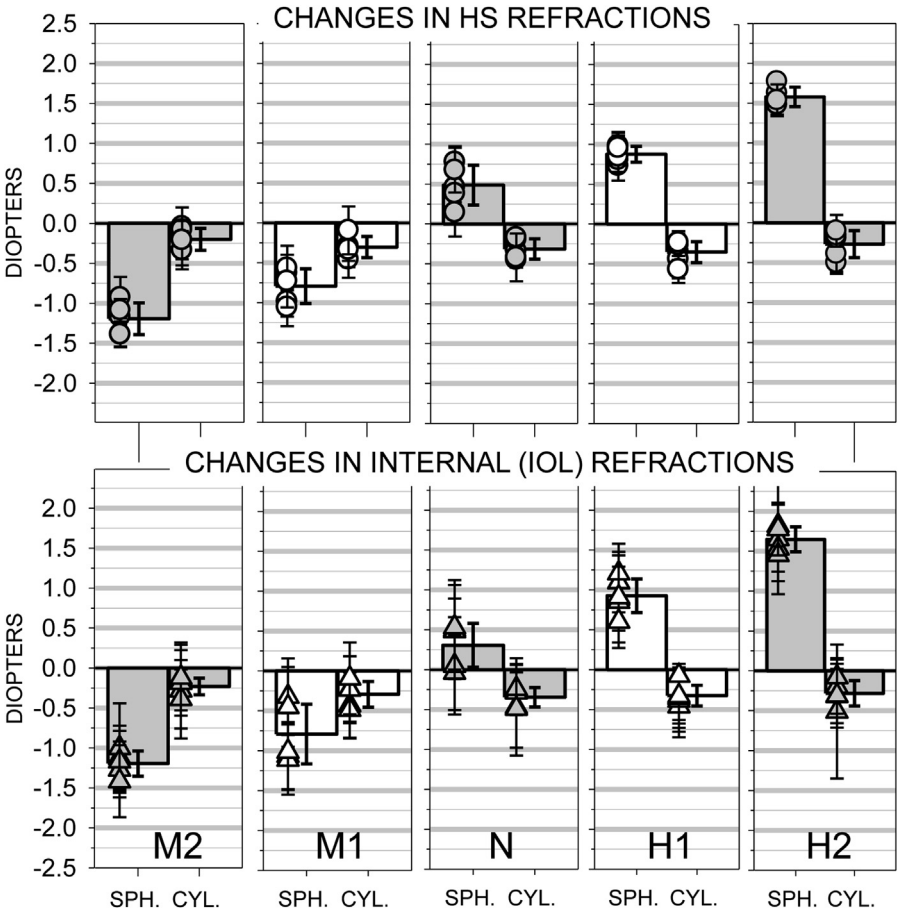

Figure 5. Refraction changes (sphere and cylinder) produced by the spherical light profiles in first adjustment, both for the whole eye (*top*) and the light-adjustable IOL (*bottom*) in vivo. Symbols express the individual data and bars the mean values (Sph. = sphere; Cyl. = cylinder; HS = Hartmann-Shack; IOL = intraocular lens; H1 and H2,= light profiles to correct hyperopia [Figure 1]; M1 and M2 = light profiles to correct myopia [Figure 1]; N = neutral light profile [Figure 1]).

adjustment. In addition to whole-eye results and to eliminate the effect of corneal changes, the internal changes (mainly due to light-adjustable IOL) are presented. All refractive changes are expressed in spherocylindrical form with negative cylinder. The mean of the experimental errors in the refraction changes in the eye and in the cornea was ±0.18 D; thus, the mean internal (IOL) error was ±0.36 D. Although the refraction changed in the expected direction in eyes treated with the same pattern, there was some variability between patients, even in the light-adjustable IOL refractive results. The mean refraction changes were similar for the eye and the IOL; the differences between them were below 0.12 D with a *P* value higher than 0.30 for all sphere and cylinder values.

Spherical profiles produced statistically significant changes in spherical powers to correct myopia and hyperopia ($P \leq .02$, except between treatments M2 and M1 for IOL calculations which was a little less significant, $P = .06$) (Table 1A and Figure 5). There was a slight hyperopic change, which induced a little myopia, with the neutral pattern. The small residual cylinder values were mainly the result of experimental and computational errors and were not statistically significant ($P \geq .26$).

Astigmatic patterns changed both components of refraction; that is, the sphere and cylinder (Table 1B and Figure 6). Two patterns corrected mixed astigmatism with the same sphere value but different amounts of cylinder. The other astigmatic profile corrected compound hyperopic astigmatism. The changes in sphere or in cylinder were significantly different between the astigmatic profiles ($P < .01$). In most eyes, the axis errors in the eye and internally were below 9 degrees (Figure 7). Thus, the efficacy of cylinder correction was higher than 70%. In particular, the MA2 profile corrected astigmatism with an accuracy of better than 5 degrees, giving an efficacy of higher than 83%.

Tables 2A and 2B show the results of the different profiles applied as a second treatment. In this case, refractive changes were between one half and one third those achieved with the first adjustment. The effect of different profiles in the second adjustment was also statistically significantly different ($P < .05$).

Lock-ins induced negligible changes in astigmatism; therefore, Tables e1, e2, and e3 (available at http://JCRS.org) show the changes in the SE power only. Although there was not a representative sample for some adjustments (eg, M2, M1, H2), in general, lock-in

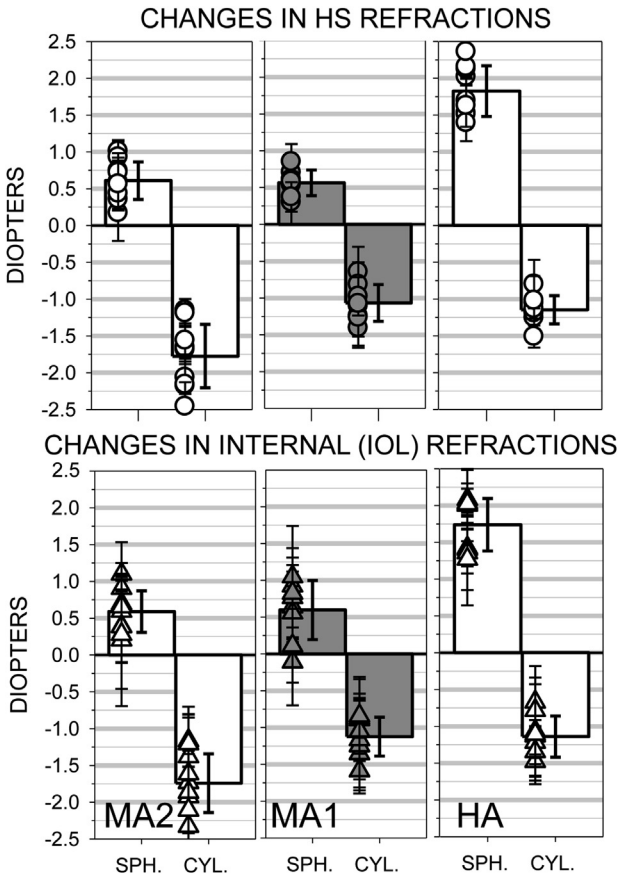

Figure 6. Refraction changes (sphere and cylinder) produced by the astigmatic light profiles in first adjustment in the eye (*top*) and the light-adjustable IOL (*bottom*). Symbols express the individual data and bars the mean values (Sph. = sphere; Cyl. = cylinder; HS = Hartmann-Shack; IOL = intraocular lens; HA = light profile to correct hyperopic astigmatism [Figure 1]; MA1 and MA2 = light profiles to correct myopic astigmatism [Figure 1]).

treatments produced a mean myopic shift of 0.33 D in eyes with 1 adjustment except in those treated with the HA profile, which was approximately 0.00 D ($P < .01$). On average, lock-in 1 induced approximately three fourths of the total myopic shift, with lock-in 2 inducing the remainder of the shift. In eyes with 2 previous adjustments, lock-ins induced a slight myopic shift (close to 0.00 D) ($P < .01$ versus eyes with 1 adjustment except with the HA pattern).

Figure e1 shows the mean change in refraction over time. The mean SE was 0.00 D. The changes in the sphere and cylinder of the IOL were negligible (<0.25 D). However, the changes, in particular in cylinder, in the eye were higher as a result of small changes in the cornea during the first year after surgery.

Figure e2 compares the subjective refraction before the first adjustment with that after the second lock-in; it shows the sphere in all eyes and the cylinder in eyes treated with astigmatic profiles in the first adjustment. As expected, spherical adjustments reduced defocus while astigmatism remained stable. Astigmatic profiles reduced sphere and cylinder at the same time. In all eyes, the mean sphere was +0.86 ± 1.16 D before the first adjustment, decreasing to +0.21 ± 0.57 D after all treatments. In eyes with astigmatic adjustments, the mean cylinder was decreased from −1.55 ± 0.36 to −0.53 ± 0.30 D; the range of the astigmatism correction was between 0.25 D and 2.00 D. The mean SE in all tested eyes before treatments was +0.28 ± 1.16 D, decreasing to −0.11 ± 0.57 D after treatments.

Figure e3 shows the decimal UDVA before treatments and after treatments. In all patients, the UDVA improved significantly with treatments. The mean was 0.64 ± 0.21 before treatments and 0.96 ± 0.19 after treatments.

DISCUSSION

Using accurate experimental approaches, we estimated the changes in refraction after light treatments

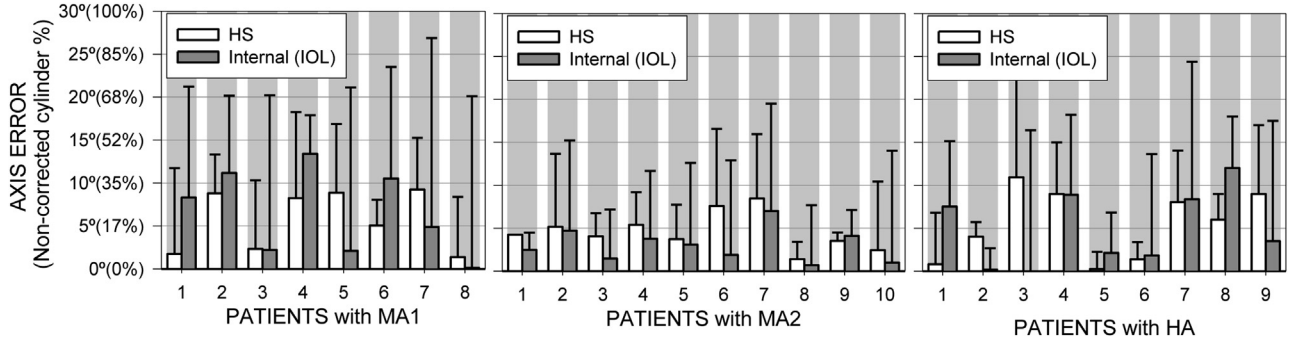

Figure 7. Orientation errors in astigmatic treatments and the uncorrected cylinder equivalent estimated in the eye and in the light-adjustable IOL (HS = Hartmann-Shack; IOL = intraocular lens; HA = light profile to correct hyperopic astigmatism [Figure 1]; MA1 and MA2 = light profiles to correct myopic astigmatism [Figure 1]).

Table 2A. Intraindividual mean values of refraction changes of the spherical profiles in the second adjustment.

Parameter	M2: 4 Samples (Mean ± SD*)	*P* Value†	N: 3 Samples (Mean ± SD*)	*P* Value†	H2: 8 Samples (Mean ± SD*)
Eye					
Sph (D)	−0.51 ± 0.14	<.01	+0.19 ± 0.09	.03	+0.69 ± 0.32
Cyl (D)	−0.21 ± 0.13	.95	−0.21 ± 0.13	.31	−0.31 ± 0.15
IOL					
Sph (D)	−0.79 ± 0.13	<.01	+0.11 ± 0.07	<.01	+0.65 ± 0.23
Cyl (D)	−0.11 ± 0.03	.20	−0.23 ± 0.14	.45	−0.31 ± 0.16

Sph = sphere; Cyl = cylinder; IOL = intraocular lens; H2 and M2 = light profiles to correct hyperopia and myopia, respectively (Figure 1); N = neutral light profile (Figure 1)
*Errors (variability) are expressed as the SD.
†Statistically significant difference between profiles is $P < .05$.

Table 2B. Intraindividual mean values of refraction changes of the astigmatic profiles in the second adjustment.

Parameter	MA2 (3 Samples) Mean ± SD*	*P* Value†	HA (3 Samples) Mean ± SD*
Eye			
Sph (D)	+0.33 ± 0.07	<.01	+0.75 ± 0.12
Cyl (D)	−1.14 ± 0.07	<.01	−0.53 ± 0.03
IOL			
Sph (D)	+0.18 ± 0.16	.04	+0.70 ± 0.26
Cyl (D)	−0.94 ± 0.18	.11	−0.57 ± 0.25

Sph = sphere; Cyl = cylinder; IOL = intraocular lens; HA = light profile to correct hyperopic astigmatism (Figure 1); MA2 = light profile to correct myopic astigmatism (Figure 1)
*Errors (variability) are expressed as the SD.
†Statistically significant difference between profiles is $P < .05$.

in eyes with the light-adjustable IOL. Objective measurements avoid common errors caused by the lack of patient cooperation during subjective measurements. During the aberration measurements, we carefully analyzed the spots of Hartmann-Shack images over the complete pupil area to detect and evaluate image problems that could affect the refractive data. Furthermore, the estimation of refraction changes with the IOL removes the possible effects resulting from corneal changes. The relatively small values of the experimental errors in objective refraction (below 0.2 D) allowed us to obtain more accurate refractive data than those measured with an autorefractor or with a subjective protocol.

Although the changes in refraction are obtained from precise measurements and calculations, the impact of the same profile on different patients is not exactly the same. For most profiles, the variability, expressed as the SD, was approximately 0.25 D. These variations could be due to different causes, which should be studied further. In preliminary measurements of the anterior chamber length using OCT, we found in some eyes slight forward axial movement of the light-adjustable IOL with the light treatments. This may explain the myopic shift after lock-in treatments and after the purely astigmatic adjustments MA1 and MA2; however, the potential axial movement of the light-adjustable IOL should be confirmed in future studies. On the other hand, there may be differences in UV transmission of the cornea between eyes, causing differences in irradiation of the light-adjustable IOL. This should also be studied; the results might lead to a custom irradiation level according to the patient's individual corneal transmission measurements.

Although the light-adjustable IOL has a UV–filtering layer on the posterior surface, limiting to safe levels the amount of UV light that reaches the retina, some patients reported mild symptoms of erythropsia in the days after the lock-in treatments. These symptoms resolved in less than 1 week in all cases. The retinal OCT examination did not show macular changes after the light treatments in any patient.

The tested patterns can correct different amounts of myopia, hyperopia, and astigmatic refractions with positive sphere. We found the light-adjustable IOL to be highly accurate inside the eye.

In this study, the final refraction and visual acuity results were good. After treatments, 80% of patients had an SE of 0.50 D or lower and 85% had astigmatism of 0.75 D or lower. The UDVA was better than 0.9 (20/22) in 70% of the treated eyes.

Light-adjustable IOLs also have the potential to modify higher-order aberrations in addition to defocus and astigmatism. A recent has study[30] found that by adding negative spherical aberration in these IOLs, it was possible to extend the depth of focus in patients. The induction of controlled aberrations together with accurate refractive outcomes will ensure optimized quality of vision.

WHAT WAS KNOWN

- Previous clinical studies report good refractive and visual acuity outcomes using light-adjustable IOLs to correct spherical and astigmatic errors up to 2.00 D after cataract surgery. However, these results could be improved if an objective and accurate method were used to determine the exact behavior of the light-adjustable IOL with different light patterns.

WHAT THIS PAPER ADDS

- The refractive changes produced by 8 light patterns (5 spherical, 3 astigmatic) and by 2 lock-in sessions used to stabilize the IOL material after light adjustments were accurately determined for the whole eye using a Hartmann-Shack sensor and for the IOL in vivo subtracting the corneal data.
- The knowledge of the accurate behavior of the light-adjustable IOL after treatment with different light patterns should improve the outcomes of this technology.

REFERENCES

1. Connors R III, Boseman P III, Olson RJ. Accuracy and reproducibility of biometry using partial coherence interferometry. J Cataract Refract Surg 2002; 28:235–238
2. Kiss B, Findl O, Menapace R, Wirtitsch M, Petternel V, Drexler W, Rainer G, Georgopoulos M, Hitzenberger CK, Fercher AF. Refractive outcome of cataract surgery using partial coherence interferometry and ultrasound biometry: clinical feasibility study of a commercial prototype II. J Cataract Refract Surg 2002; 28:230–234
3. Rajan MS, Keilhorn I, Bell JA. Partial coherence laser interferometry vs conventional ultrasound biometry in intraocular lens power calculations. Eye 2002; 16:552–556. Available at: http://www.nature.com/eye/journal/v16/n5/pdf/6700157a.pdf. Accessed March 11, 2014
4. Narváez J, Zimmerman G, Stulting RD, Chang DH. Accuracy of intraocular lens power prediction using the Hoffer Q, Holladay 1, Holladay 2, and SRK/T formulas. J Cataract Refract Surg 2006; 32:2050–2053
5. Wang J-K, Hu C-Y, Chang S-W. Intraocular lens power calculation using the IOLMaster and various formulas in eyes with long axial length. J Cataract Refract Surg 2008; 34:262–267
6. Haigis W. Intraocular lens calculation after refractive surgery for myopia: Haigis-L formula. J Cataract Refract Surg 2008; 34:1658–1663
7. Canovas C, Artal P. Customized eye models for determining optimized intraocular lenses power. Biomed Opt Express 2011; 2:1649–1662. Available at: http://www.ncbi.nlm.nih.gov/pmc/articles/PMC3114231/pdf/1649.pdf. Accessed March 11, 2014
8. Canovas C, Abenza S, Alcon E, Villegas EA, Marin JM, Artal P. Effect of corneal aberrations on intraocular lens power calculations. J Cataract Refract Surg 2012; 38:1325–1332
9. Özkurt Y, Erdoğan G, Güveli AK, Oral Y, Özbaş M, Çömez AT, Doğan ÖK. Astigmatism after superonasal and superotemporal clear corneal incisions in phacoemulsification. Int Ophthalmol 2008; 28:329–332
10. Barequet IS, Yu E, Vitale S, Cassard S, Azar DT, Stark WJ. Astigmatism outcomes of horizontal temporal versus nasal clear corneal incision cataract surgery. J Cataract Refract Surg 2004; 30:418–423
11. Hoffer KJ. Biometry of 7,500 cataractous eyes. Am J Ophthalmol 1980; 90:360–368; correction, 890
12. Jiang Y, Le Q, Yang J, Lu Y. Changes in corneal astigmatism and high order aberrations after clear corneal tunnel phacoemulsification guided by corneal topography. J Refract Surg 2006; 22:S1083–S1088
13. Guirao A, Tejedor J, Artal P. Corneal aberrations before and after small-incision cataract surgery. Invest Ophthalmol Vis Sci 2004; 45:4312–4319. Available at: http://www.iovs.org/cgi/reprint/45/12/4312. Accessed March 11, 2014
14. Khokhar S, Lohiya P, Murugiesan V, Panda A. Corneal astigmatism correction with opposite clear corneal incisions or single clear corneal incision: comparative analysis. J Cataract Refract Surg 2006; 32:1432–1437
15. Sun X-Y, Vicary D, Montgomery P, Griffiths M. Toric intraocular lenses for correcting astigmatism in 130 eyes. Ophthalmology 2000; 107:1776–1781; discussion by RM Kershner, 1781–1782
16. Bauer NJ, de Vries NE, Webers CA, Hendrikse F, Nuijts RM. Astigmatism management in cataract surgery with the AcrySof toric intraocular lens. J Cataract Refract Surg 2008; 34:1483–1488
17. Mendicute J, Irigoyen C, Aramberri J, Ondarra A, Montés-Micó R. Foldable toric intraocular lens for astigmatism correction in cataract patients. J Cataract Refract Surg 2008; 34:601–607
18. Schwartz DM. Light-adjustable lens. Trans Am Ophthalmol Soc 2003; 101:417–436. Available at: http://www.ncbi.nlm.nih.gov/pmc/articles/PMC1358999/pdf/14971588.pdf. Accessed March 11, 2014
19. Schwartz DM, Sandstedt CA, Chang SH, Kornfield JA, Grubbs RH. Light-adjustable lens: development of in vitro nomograms. Trans Am Ophthalmol Soc 2004; 102:67–72. discussion 72–74. Available at: http://www.ncbi.nlm.nih.gov/pmc/articles/PMC1280088/pdf/tao102pg067.pdf. Accessed March 11, 2014
20. Chayet A, Sandstedt C, Chang S, Rhee P, Tsuchiyama B, Grubbs R, Schwartz D. Correction of myopia after cataract surgery with a light-adjustable lens. Ophthalmology 2009; 116:1432–1435
21. Chayet A, Sandstedt CA, Chang SH, Rhee P, Tsuchiyama B, Schwartz D. Correction of residual hyperopia after cataract surgery using the light adjustable lens technology. Am J Ophthalmol 2009; 147:392–397
22. Hengerer FH, Dick HB, Conrad-Hengerer I. Clinical evaluation of an ultraviolet light adjustable intraocular lens implanted after cataract removal; eighteen months follow-up. Ophthalmology 2011; 118:2382–2388
23. Chayet A, Sandstedt C, Chang S, Rhee P, Tsuchiyama B, Grubbs R, Schwartz D. Use of the light-adjustable lens to correct astigmatism after cataract surgery. Br J Ophthalmol 2010; 94:690–692
24. Sandstedt CA, Chang SH, Grubbs RH, Schwartz DM. Light-adjustable lens: customizing correction for multifocality and higher-order aberrations. Trans Am Ophthalmol Soc 2006; 104:29–38. discussion 38–39. Available at: http://www.ncbi.nlm.nih.gov/pmc/articles/PMC1809908/pdf/1545-6110_v104_p029.pdf. Accessed March 11, 2014
25. Prieto PM, Vargas-Martín F, Goelz S, Artal P. Analysis of the performance of the Hartmann-Shack sensor in the human eye. J Opt Soc Am A Opt Image Sci Vis 2000; 17:1388–1398

26. Artal P, Benito A, Tabernero J. The human eye is an example of robust optical design. J Vis 2006; 6:1–7. Available at: http://www.journalofvision.org/content/6/1/1.full.pdf. Accessed March 11, 2014
27. Guirao A, Artal P. Corneal wave aberration from videokeratography: accuracy and limitations of the procedure. J Opt Soc Am A Opt Image Sci Vis 2000; 17:955–965
28. Artal P. Combining corneal and ocular wave-aberrations. In: Krueger RR, Applegate RA, MacRae S, eds, Wavefront Customized Visual Correction; The Quest for Super Vision II. Thorofare, NJ, Slack, 2004; 311–316
29. American National Standards Institute, Inc. American National Standards for Ophthalmics – Methods for Reporting Optical Aberrations of Eyes. New York, NY, ANSI Z80.28, 2004
30. Villegas EA, Alcón E, Mirabet S, Yago I, Marín JM, Artal P. Extended depth of focus with induced spherical aberration in light-adjustable intraocular lenses. Am J Ophthalmol 2014; 157:142–149

First author:
Eloy A. Villegas, PhD

Laboratorio de Optica, Departamento de Física, Universidad de Murcia, Spain

Table e1. Intraindividual mean values of SE changes with lock-ins after 1 spherical adjustment.

	Mean (D) ± SD*				
Parameter	M2: 2 Samples	M1: 2 Samples	N: 3 Samples	H1: 6 Samples	H2: 2 Samples
Eye	+0.47 ± 0.11	+0.38 ± 0.07	+0.64 ± 0.19	+0.37 ± 0.13	+0.14 ± 0.23
IOL	+0.20 ± 0.04	+0.34 ± 0.20	+0.57 ± 0.28	+0.39 ± 0.23	+0.02 ± 0.08

IOL = intraocular lens; H1 and H2 = light profiles to correct hyperopia (Figure 1); M1 and M2 = light profiles to correct myopia (Figure 1); N = neutral light profile (Figure 1)
*Errors (variability) are expressed as the SD.

Table e2. Intraindividual mean values of SE changes with lock-ins after 1 astigmatic adjustment.

	Mean (D) ± SD*		
Parameter	MA2: 3 Samples	MA1: 6 Samples	HA: 4 Samples
Eye	+0.41 ± 0.11	+0.31 ± 0.20	−0.02 ± 0.11
IOL	+0.37 ± 0.25	+0.24 ± 0.22	+0.01 ± 0.11

IOL = intraocular lens; HA = light profile to correct hyperopic astigmatism (Figure 1); MA1 and MA2 = light profiles to correct myopic astigmatism (Figure 1)
*Errors (variability) are expressed as the SD.

Table e3. Intraindividual mean values of SE changes with lock-ins after 2 adjustments.

Parameter	25 Samples (Mean (D) ± SD*)
Eye	+0.06 ± 0.23
IOL	+0.16 ± 0.16

IOL = intraocular lens
*Errors (variability) are expressed as the SD.

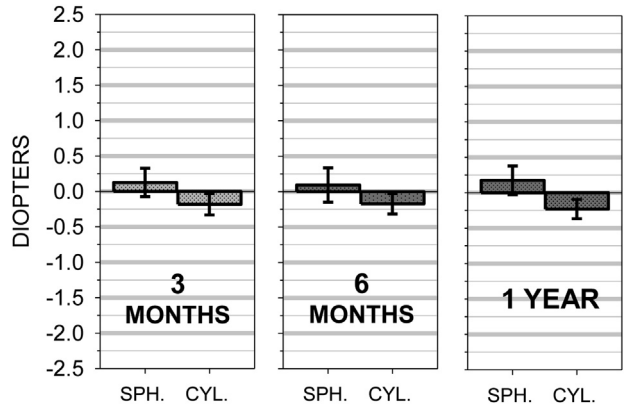

Figure e1. The mean changes in the eye and light-adjustable IOL refractions between second lock-in and 3 months, 6-month, and 1 year (Cyl. = cylinder; Sph. = sphere).

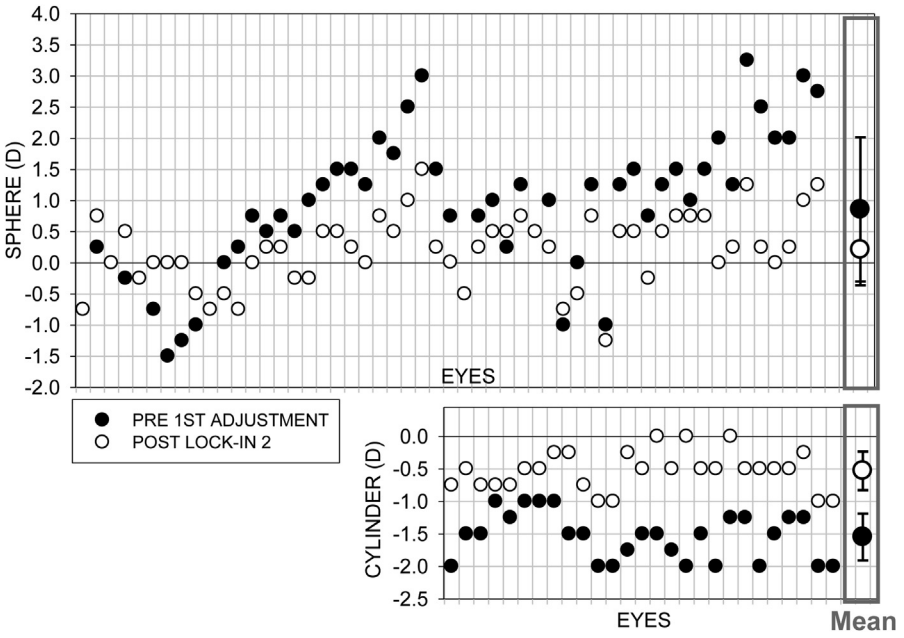

Figure e2. Manifest refraction before the first adjustment and after the second lock-in; sphere in all tested eyes and cylinder in eyes treated with astigmatic profiles in the first adjustment.

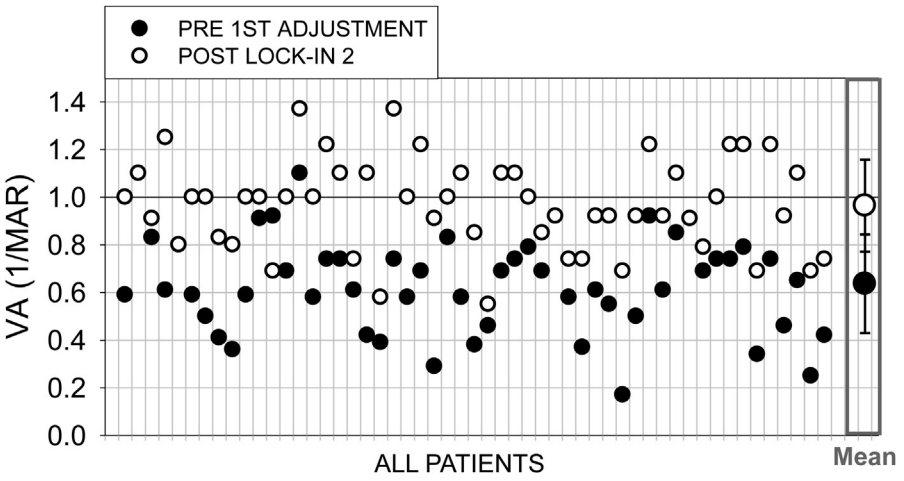

Figure e3. Uncorrected distance visual acuity (decimal scale) before first adjustment and after second lock-in (VA = uncorrected distance visual acuity).